Laser and Particle Beams (2012), *30*, 307–311.

doi:10.1017/S0263034612000134

Improvement of proton energy in high-intensity laser-nanobrush target interactions

JINQING YU,[1,2] WEIMIN ZHOU,[2] XIAOLIN JIN,[1] LIHUA CAO,[3] ZONGQING ZHAO,[2] WEI HONG,[2] BIN LI,[1] AND YUQIU GU[2]

[1]University of Electronic Science and Technology of China, Chengdu, China
[2]Research Center of Laser Fusion, China Academy of Engineering Physics, Mianyang, China
[3]Institute of Applied Physics and Computational Mathematics, Beijing, China.

(Received 8 September 2011; Accepted 13 February 2012)

Abstract

In order to improve the total laser-proton energy conversion efficiency, a nanobrush target is proposed for proton acceleration and investigated by two-dimensional particle-in-cell simulation. The simulation results show that the nanobrush target significantly enhances the energy and number of hot electrons through the target rear side. Compared with plain target, the sheath field on the rear surface is increased near 100% and the total laser-proton energy conversion efficiency is prompted more than 70%. Furthermore, the proton divergence angle is less than 30° by using nanobrush target. The proposed target may serve as a new method to increase the energy conversion efficiency from laser to protons.

Keywords: Energy conversion efficiency; Nanobrush target; Particle-in-cell; Proton divergence angle; Sheath field

1. INTRODUCTION

When an ultra-intense laser pulse irradiates on a solid target, relativistic electrons are generated at the interface (Cai *et al.*, 2009). The hot electrons move forward through the plasma-vacuum interface and create a space-charge field in the target rear side. The strong electrostatic field plumbs to the rear and accelerates protons to high energies. This mechanism is well known as "target normal sheath acceleration" (TNSA) (Wilks *et al.*, 2001). The TNSA is one of the major proton acceleration mechanisms. Laser-plasma driven proton beam has significant and peculiar characteristics, and is widely used in diagnostics of high energy density physics (Borghesi *et al.*, 2002; Li *et al.*, 2009, 2008; Romagnani *et al.*, 2008), inertial confinement fusion (Roth *et al.*, 2001; Deutsch, 2003), and other fields (Limpouch *et al.*, 2008; Andreev *et al.*, 2009; Offermann *et al.*, 2009). Actually, the energy-conversion efficiency from laser to proton is very low. One of the major reasons is that a significant part of laser energy is reflected by the surface of thin-foil target (Nodera *et al.*, 2008).

Some novel structured targets have been proposed to reduce the reflection and enhance the absorption of intense short-pulse laser, including sub-wavelength nano-layered target (Cao *et al.*, 2010*a*, 2010*b*; Ji *et al.*, 2010; Zhao *et al.*, 2010), sub-λ gratings (Kahaly *et al.*, 2008), nano-structured "velvet" targets (Kulcsár *et al.*, 2000), and micro-structured targets (Klimo *et al.*, 2011). A monolayer of polystyrene microspheres of a size similar to the laser wavelength on the front surface of a thin foil has been proposed to construct the target for ion acceleration experiments (Klimo *et al.*, 2011). The reflection of the laser energy can be reduced and the absorption can be increased by using the target with sub-wavelength nanolayered front. The laser energy absorption can reach near-100% in the scheme of sub-λ gratings (Kahaly *et al.*, 2008). By using the sub-wavelength nanolayered target (Cao *et al.*, 2010*a*, 2010*b*), the absorption of laser energy can reach more than 80% and the reflection is less than 10%.

In this paper, a nanobrush target is proposed to accelerate proton and improve the quantity of accelerated protons. Since the sub-wavelength nanolayered structure is beneficial in enhancing the laser absorption, decreasing the divergence of hot electron, and increasing the yield of forward hot electron (Cao *et al.*, 2010*a*). The nanobrush target is consisted of a sub-wavelength nanolayered adhibitted to the front of a plain targets. The proton acceleration is investigated by two-dimensional particle-in-cell code Flips2d, which has been successfully used to investigate the laser-plasma interactions

Address correspondence and reprint requests to: Yuqiu Gu; National Key Laboratory of Laser Fusion, Research Center of Laser Fusion, China Academy of Engineering Physics, P.O. Box, 919-986, Mianyang, Sichuan Province, China 621900. E-mail: yqgu@caep.ac.cn

(Zhou *et al.*, 2008, 2010). The simulation results show that the number of hot electron through the rear side of the target and the sheath field there can be enhanced significantly by using the nanobrush target. Compared with the plain target, the total laser-proton energy conversion efficiency can be enhanced more than 70% and the proton divergence angle is less than 30°. This paper is organized as follows. In Section 2, the simulation model is introduced and the simulation results of the two targets will be presented in Section 3. The results are finally summarized in Section 4.

2. SIMULATION MODEL

The scale of simulation box used here is $X_L \times Y_L = 50\lambda_0 \times 30\lambda_0$, the time step is chosen as 0.0125τ, the simulation duration is 200τ and the grid sizes are $\Delta X = \Delta Y = 0.025\lambda_0$, where τ and $\lambda_0 = 1.06$ μm are the period and wavelength of laser pulse, respectively. We considered a laser pulse with Gaussian profile in the y direction. A p-polarized laser pulse with a focal spot of $4\lambda_0$ introduces along the axis from the left. The pulse shape in the x direction is assumed to rise up to the peak intensity in 5τ, maintain at the peak intensity for 20τ, and then fall down to zero in another 5τ. The peak intensity is $I_0 = 3.5 \times 10^{19}$ W/cm^2. The initial temperatures of electrons and ions are both 1.0 keV. A plain target and a nanobrush target are schemed in Figure 1. The plain target is $1.0\lambda_0$ length $8.0\lambda_0$ wide. In the case of nanobrush target, the plain target is $0.5\lambda_0$ in length $8.0\lambda_{0\ \mathrm{in}}$ wide, and a $0.5\lambda_0$ length nanolayered target is adhibitted to the front of the plain target. The plain target is used to support the nanolayered target and adjust the state of hot electrons beams through the rear. The width and the interlayer vacuum spacing of the nanolayered target are $0.1\lambda_0$ and $0.4\lambda_0$, respectively. The width of the layer and the interlayer vacuum spacing are considered to be the optimization for achieving small reflectivity and large absorptive (Cao *et al.*, 2010*a*). The hydrogen targets with $0.2\lambda_0$ thick and $4\lambda_0$ wide are adhibitted to the backs of high-Z material targets. Both the plain target and the nanobrush target of high-Z material are assumed to Al^{3+} plasma with the density of $20n_c$, where n_c is the critical density, which is related to the frequency of the laser as $n_c = m_e\omega_0^2/4\pi e^2$. The density of the hydrogen layer is n_c. The number of the particle per cell is 225 electrons and 25 ions for high-Z material, 225 electrons and 225 protons for hydrogen layer. In the following description, the normalized electron field and magnetic field are given.

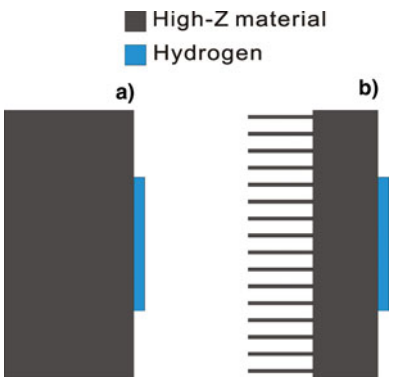

Fig. 1. (Color online) Target configurations, (**a**) the plain target, (**b**) the nanobrush target. The plain target and the nanobrush target are high-Z material with the density of $20n_c$, but the density of the hydrogen layers is n_c.

3. NUMERICAL SIMULATION RESULT

The peak value of the electrostatic charge-separation field in the target rear side can be described as $E = \sqrt{2}k_BT_e/e\lambda_D$ (Mora *et al.*, 2003, 2005), where k_B is Boltzmann constant, T_e is electron temperature, and λ_D is the electron Debye length in the rear surface, and e denotes the numerical constant. The relation between λ_D and the initial Debye length λ_{D0} is $\lambda_D = \lambda_{D0}\ (n_{e0}/n_e)^{1/2}$, where n_{e0} and n_e are electron density in the unperturbed and on the rear, respectively. Thus we can obtain $E \propto n_e^{1/2}$, which implies that the electric field can be enhanced by increasing n_e.

Figure 2 shows the energy spectrums of hot electrons of the plain target and the nanobrush target in 60τ. Only the hot electrons (0.5 MeV–5.0 MeV) with forward velocity through the rear side are included. One can see that larger number of hotter electrons can be achieved by using the nanobrush target, which will result in the enhancement of the sheath field in the target rear surface.

From the above result, the number of hot electrons n_e passing through the rear surface can be enhanced by using the nanobrush target. From the relation of $E \propto n_e^{1/2}$, the sheath field in the rear surface will be enhanced as the encroachment of n_e. Figure 3a shows the sheath field distribution in the y direction $0.0125\lambda_0$ beyond the rear surface of the two targets at 40τ. One can see that the sheath field has been enhanced near a time by using the nanobrush target. Figure 3b shows the Ex-distribution in the x direction of the two targets at 40τ. The peak value of the electrostatic charge-separation field on the target rear has also been enhanced a times. From the above analysis and the simulation results, it is observed that the sheath field of the nanobrush target is larger than that of the plain target.

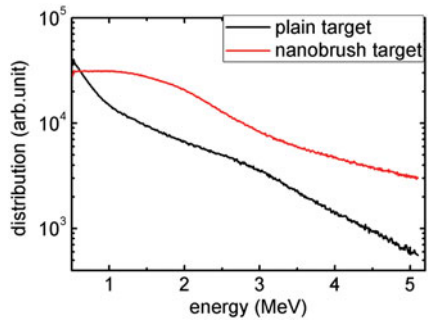

Fig. 2. (Color online) Energy spectrums of hot electrons through the rear sides of the two targets. Only the hot electrons (0.5 MeV–5.0 MeV) with forward velocity through the rear surface in 60τ are included.

https://doi.org/10.1017/S0263034612000134 Published online by Cambridge University Press

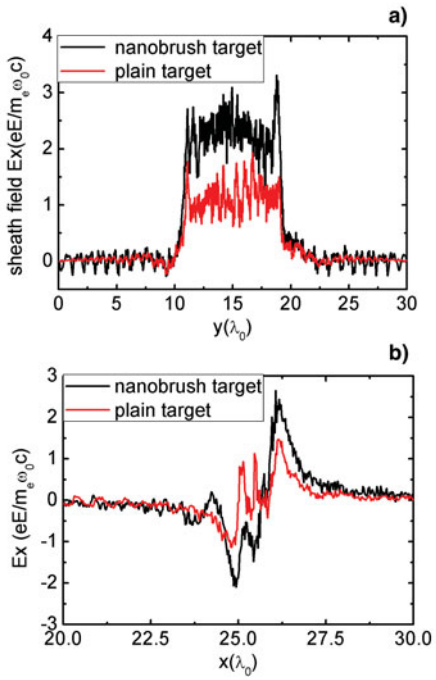

Fig. 3. (Color online) The electric field Ex distributions at 40τ: (**a**) sheath field distribution in y direction $0.0125\lambda_0$ beyond the rear surfaces of the two targets; (**b**) Ex distribution on the laser axis.

Now we are concentrating to investigate the energy conversion from the laser to the protons. Figure 4 shows the time dependence of the total-energy of protons for these two kinds of targets. It is shown that the proton total-energy peaks at the time of 160τ, and the total laser-proton energy conversion efficiency can be enhanced more than 70% compared with the plain target. It is resulted from both the high efficient absorption and the enhancement of electrostatic field in the target rear side.

Figure 5 shows the proton kinetic energy distributions of the two targets at the time of 160τ. The maximum and minimum proton energies are, respectively, 20.2 MeV and 3.5 MeV in the case of the nanobrush target, but they are 16.1

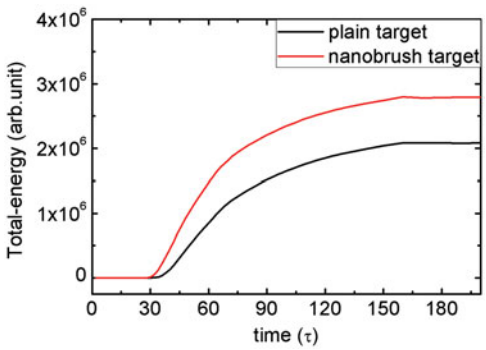

Fig. 4. (Color online) Total-energy histories of protons, the proton total-energy can reach the peak value at 160τ.

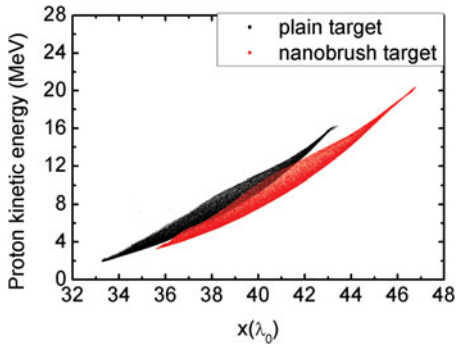

Fig. 5. (Color online) Proton kinetic energy distributions of the two targets at time of 160τ. The average proton energies are 9.66 MeV for the nanobrush target and 7.24 MeV for the plain target, respectively.

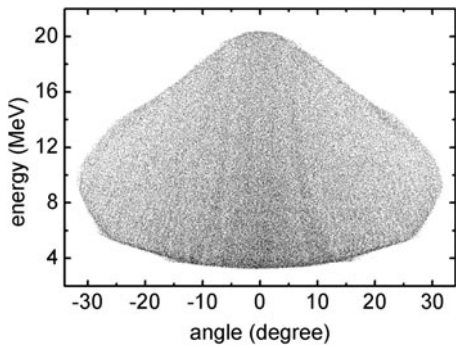

Fig. 6. The relation between proton energy and divergence angle at 160τ.

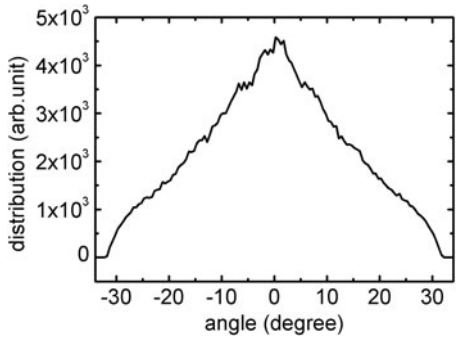

Fig. 7. Proton divergence angle of nanobrush target at 160τ. The divergence angle is 29.52°.

MeV and 2.0 MeV under the condition of the plain target. Furthermore, the average proton energies can be estimated to be 9.66 MeV for the nanobrush target and 7.24 MeV for the plain target. It means the average proton energy has been enhanced more than 70% by using the nanobrush target.

We now discuss the divergence of the accelerated protons. Figure 6 shows the relation between proton energy and divergence angle at the time of 160τ. It is shown that the higher energy the protons have the smaller divergence angle the protons achieve. Figure 7 shows the divergence angle

https://doi.org/10.1017/S0263034612000134 Published online by Cambridge University Press

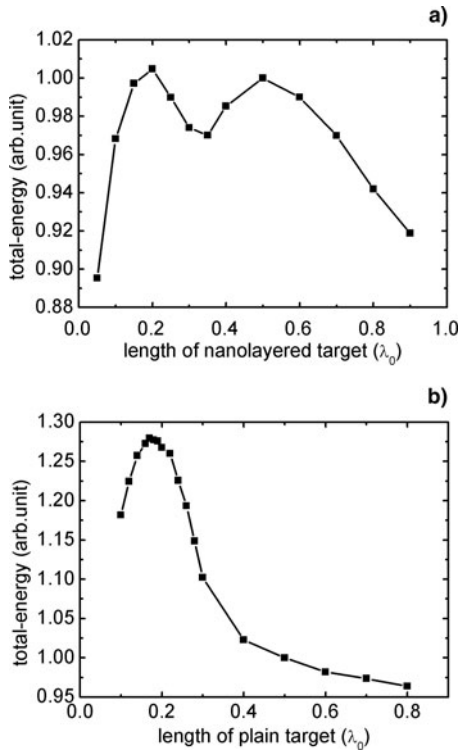

Fig. 8. Dependence of the proton total-energy on the length of the nanolayered target and plain target, the value of 1 denotes the case of the nanobrush target with $0.5\lambda_0$ length nanolayered target and $0.5\lambda_0$ length plain target, (**a**) the relation between the proton total-energy and the length of nanolayered target with the length of the plain target to be $0.5\lambda_0$, (**b**) the relation of the proton total-energy and the plain target with $0.5\lambda_0$ length of nanolayered target.

distribution of the protons in the transverse direction of nanobrush target at the time of 160τ, from which we can get a divergence angle of $\theta_{FWHM} = 29.52°$.

Figure 8 shows the dependence of the proton total-energy on the length of the nanolayered target and plain target. The value of 1 is the case that the proton total-energy of the nanobrush target with the lengths of the nanolayered target and the plain target are both $0.5\lambda_0$. In Figure 8a, one can see that the effect of the length of nanolayered target on the proton total-energy is very weak with the length between $0.1\lambda_0$ and $0.7\lambda_0$. If the length is shorter or longer, the effect will become very strong. From Figure 8b, we can find that the proton total-energy dependences on the length plain very significant and can be enhanced about 28% with the plain target of $0.7\lambda_0$.

4. CONCLUSION

A nanobrush target is proposed to improve the laser-proton energy conversion efficiency. Two-dimensional particle-in-cell simulation results show that larger number of the hot electrons through the rear surface can be achieved by using the nanobrush target compared with plain target. The peak value of the electrostatic charge-separation field in the target rear side is related to the number of hot electrons through the rear surface. Compared with the plain target, the field increases several times since more electrons carrying larger energies pass through the rear side. By optimizing the sizes of the nanolayered target, the average proton energy can be enhanced more than 70% and the total laser-proton energy conversion efficiency can also be enhanced more than 70%. In addition, the proton divergence angle is less than 30°. With the proposed nanobrush target, more energetic protons with smaller divergence can be generated more efficiently. It can thus be useful as a source of collimated protons for various applications.

ACKNOWLEDGMENTS

This work is supported by the National Natural Science Foundation of China (Grant Nos. 10905009, 11174259, 11175030, 11175165, and 10975121), the Doctorate Foundation of the Ministry of Education of China (Grant No. 200806141034), the Fundamental Research Funds for the Central Universities (Grant No. ZYGX2010J052), the National High-Tech Committee and the National Key Laboratory of Laser Fusion (Grant No. 9140c6802031003).

REFERENCES

Andreev, A.A., Steinke, S., Sokollik, T., Schnurer, M., Ter Avetsiyan, S., Platonov, K.Y. & Nickles, P.V. (2009). Optimal ion acceleration from ultrathin foils irradiated by a profiled laser pulse of relativistic intensity. *Phys. Plasmas* **16**, 013103–9.

Borghesi, M., Campbell, D.H., Schiavi, A., Willi, O., Mackinnon, A.J., Hicks, D., Patel, P., Gizzi, L.A., Galimberti, M. & Clarke, R.J. (2002). Laser-produced protons and their application as a particle probe. *Laser Part. Beams* **20**, 269–275.

Cai, H.B., Mima, K., Zhou, W.M., Jozaki, T., Nagatomo, H., Sunahara, A. & Mason, R.J. (2009). Enhancing the number of high-energy electrons deposited to a compressed pellet via double cones in fast ignition. *Phys. Rev. Lett.* **102**, 245001–4.

Cao, L.H., Gu, Y.Q., Zhao, Z.Q., Cao, L.F., Huang, W.Z., Zhou, W.M., Cai, H.B., He, X.T., Yu, W. & Yu, M.Y. (2010*a*). Enhanced absorption of intense short-pulse laser light by subwavelength nanolayered target. *Phys. Plasmas* **17**, 103106–6.

Cao, L.H., Gu, Y.Q., Zhao, Z.Q., Cao, L.F., Huang, W.Z., Zhou, W.M., He, X.T., Yu, W. & Yu, M.Y. (2010b). Control of the hot electrons produced by laser interaction with nanolayered target. *Phys. Plasmas* **17**, 043103–6.

Deutsch, C. (2003). Transport of mega electron volt protons for fast ignition. *Laser Part. Beams* **21**, 70–35.

Ji, Y.L., Jiang, G.W., Wu, D., Wang, C.Y., Gu, Y.Q. & Tang, Y.J. (2010). Efficient generation and transportation of energetic electrons in a carbon nanotube array target. *Appl. Phys. Lett.* **96**, 041504–3.

Kahaly, Subhendu, Yadav, S.K., Wang, W.M., Sengupta, S., Sheng, Z.M., Das, A., Kaw, P.K. & Kumar, G.R. (2008). Near-complete absorption of intense, ultrashort laser light by sublambda gratings. *Phys. Rev. Lett.* **101**, 145001–4.

Klimo, O., Psikal, J., Limpouch, J., Proska, J., Novotny, F., Ceccotti, T., Floquet, V. & Kawata, S. (2011). Short pulse laser

https://doi.org/10.1017/S0263034612000134 Published online by Cambridge University Press

interaction with micro-structured targets: Simulations of laser absorption and ion acceleration. *New J. Phys*. **13**, 053028–17.

Kulcsár, G., AlMawlawi, D., Budnik, F.W., Herman, P.R., Moskovits, Zhao, M.L. & Marjoribanks, R.S. (2000). Intense picosecond x-ray pulses from laser plasmas by use of nanostructured "velvet" targets. *Phys. Rev. Lett*. **84**, 5149–4.

Li, C.K., Seguin, F.H., Frenje, J.A., Manuel, M., Casey, D., Sinenian, N., Petrasso, R.D., Amendt, P.A., Landen, O.L., Rygg, J.R., Town, R.P.J., Betti, R., Delettrez, J., Knauer, J.P., Marshall, F., Meyerhofer, D.D., Sangster, T.C., Shvarts, D., Smalyuk, V.A., Soures, J.M., Back, C.A., Kilkenny, J.D. & Nikroo, A. (2009). Proton radiography of dynamic electric and magnetic fields in laser-produced high-energy-density plasmas. *Phys. Plasmas* **16**, 056304–6.

Li, X.M., Shen, B.F., Zhang, X.M., Jin, Z.Y. & Wang, F.C. (2008). The diagnostics of density distribution for inhomogeneous dense DT plasmas using fast protons. *Laser Part. Beams* **26**, 139–145.

Limpouch, J., Psikal, J., Andreev, A.A., Platonov, K.Y. & Kawata, S. (2008). Enhanced laser ion acceleration from mass-limited targets. *Laser Part. Beams* **26**, 225–234.

Mora, P. (2003). Plasma expansion into a vacuum. *Phys. Rev. Lett*. **90**, 185002–4.

Mora, P. (2005). Thin-foil expansion into a vacuum. *Phys. Rev. E*. **72**, 056401–5.

Nodera, Y., Kawata, S., Onuma, N., Limpouch, J., Klimo, O. & Kikuchi, T. (2008). Improvement of energy-conversion efficiency from laser to proton beam in a laser-foil interaction. *Phys. Rev. E*. **78**, 046401–6.

Offermann, D.T., Freeman, R.R., Van Woerkom, L.D., Foord, M.E., Hey, D., Key, M.H., Mackinnon, A.J., MacPhee, A.G., Patel, P.K., Ping, Y., Sanchez, J.J., Shen, N., Bartal, T., Beg, F.N., Espada, L., Chen, C.D. (2009). Observations of proton beam enhancement due to erbium hydride on gold foil targets. *Phys. Plasmas* **16**, 093113–7.

Romagnani, L., Borghesi, M., Cecchetti, C.A., Kar, S., Antici, P., Audebert, P., Bandhoupadjay, S., Ceccherini, F., Cowan, T., Fuchs, J., Galimberti, M., Gizzi, L.A., Grismayer, T., Heathcote, R., Jung, R., Liseykina, T.V., Macchi, A., Mora, P., Neely, D., Notley, M., Osterholtz, J., Pipahl, C.A., Pretzler, G., Schiavi, A., Schurtz, G., Toncian, T., Wilson, P.A. & Willi, O. (2008). Proton probing measurement of electric and magnetic fields generated by ns and ps laser-matter interactions. *Laser Part. Beams* **26**, 241–248.

Roth, M., Cowan, T.E., Key, M.H., Hatchett, S.P., Brown, C., Fountain, W., Johnson, J., Pennington, D.M., Snavely, R.A., Wilks, S.C., Yasuike, K., Ruhl, H., Pegoraro, F., Bulanov, S.V., Campbell, E.M., Perry, M.D. & Powell, H. (2001). Fast ignition by intense laser-accelerated proton beams. *Phys. Rev. Lett*. **86**, 436–439.

Wilks, S.C., Langdon, A.B., Cowan, T.E., Roth, M., Singh, M., Hatchett, S., Key, M.H., Pennington, D., MacKinnon, A. & Snavely, R.A. (2001). Energetic proton generation in ultra-intense laser–solid interactions. *Phys. Plasmas* **8**, 542–549.

Zhao, Z.Q., Cao, L.H., Cao, L.F., Wang, J., Huang, W.Z., Jiang, W., He, Y.L., Wu, Y.C., Zhu, B., Dong, K.G., Ding, Y.K., Zhang, B.H., Gu, Y.Q., Yu, M.Y. & He, X.T. (2010). Acceleration and guiding of fast electrons by a nanobrush target. *Phys. Plasmas* **17**, 123108.

Zhou, W.M., Gu, Y.Q., Hong, W., Zhao, Z.Q., Ding, Y.K., Zhang, B.H., Cai, H.B. & Mima, K. (2010). Enhancement of monoenergetic proton beams via cone substrate in high intensity laser pulse-double layer target interactions. *Laser Part. Beams* **28**, 585–590.

Zhou, W.M., Mima, K., Nakamura, T. & Nagatomo, H. (2008). Probing of nonlinear evolution of laser Wakefield by Raman scattering of laser light. *Phys. Plasmas* **15**, 093107–6.

https://doi.org/10.1017/S0263034612000134 Published online by Cambridge University Press